Interacting-heads motif has been conserved as a mechanism of myosin II inhibition since before the origin of animals

Kyoung Hwan Lee[a,1,2], Guidenn Sulbarán[a,b,1,3], Shixin Yang[a,2], Ji Young Mun[a,4], Lorenzo Alamo[b], Antonio Pinto[b], Osamu Sato[c], Mitsuo Ikebe[c], Xiong Liu[d], Edward D. Korn[d], Floyd Sarsoza[e], Sanford I. Bernstein[e], Raúl Padrón[b,5], and Roger Craig[a,2,5]

[a]Department of Cell and Developmental Biology, University of Massachusetts Medical School, Worcester, MA 01655; [b]Centro de Biología Estructural, Instituto Venezolano de Investigaciones Científicas, 1020A Caracas, Venezuela; [c]Department of Cellular and Molecular Biology, University of Texas Health Science Center at Tyler, Tyler, TX 75708; [d]Laboratory of Cell Biology, National Heart, Lung, and Blood Institute, National Institutes of Health, Bethesda, MD 20892; and [e]Department of Biology, San Diego State University, San Diego, CA 92182

Electron microscope studies have shown that the switched-off state of myosin II in muscle involves intramolecular interaction between the two heads of myosin and between one head and the tail. The interaction, seen in both myosin filaments and isolated molecules, inhibits activity by blocking actin-binding and ATPase sites on myosin. This interacting-heads motif is highly conserved, occurring in invertebrates and vertebrates, in striated, smooth, and nonmuscle myosin IIs, and in myosins regulated by both Ca^{2+} binding and regulatory light-chain phosphorylation. Our goal was to determine how early this motif arose by studying the structure of inhibited myosin II molecules from primitive animals and from earlier, unicellular species that predate animals. Myosin II from *Cnidaria* (sea anemones, jellyfish), the most primitive animals with muscles, and *Porifera* (sponges), the most primitive of all animals (lacking muscle tissue) showed the same interacting-heads structure as myosins from higher animals, confirming the early origin of the motif. The social amoeba *Dictyostelium discoideum* showed a similar, but modified, version of the motif, while the amoeba *Acanthamoeba castellanii* and fission yeast (*Schizosaccharomyces pombe*) showed no head–head interaction, consistent with the different sequences and regulatory mechanisms of these myosins compared with animal myosin IIs. Our results suggest that head–head/head–tail interactions have been conserved, with slight modifications, as a mechanism for regulating myosin II activity from the emergence of the first animals and before. The early origins of these interactions highlight their importance in generating the inhibited (relaxed) state of myosin in muscle and nonmuscle cells.

interacting-heads motif | myosin II | evolution | myosin regulation | muscle

Myosin II is the motor protein that constitutes the thick filaments of muscles where, by interacting with the thin (actin-containing) filaments, it brings about ATP-powered muscular contraction in animals (1). Myosin II is also present in nonmuscle cells of animals and in organisms that predate animal evolution (e.g., fungi, amoebae), where, together with actin, it functions in cell division, cell migration, endocytosis and exocytosis, and changes in cell shape. Myosin II consists of two identical heavy chains and two pairs of light chains, which together form a two-headed molecule with an elongated tail (2). The C-terminal halves of the heavy chains are α-helical and wrap around each other to form the tail, while the N-terminal halves form the globular heads. The heads each consist of a motor domain, which hydrolyzes ATP and binds to actin, and a light-chain domain containing a regulatory light chain (RLC) and an essential light chain (ELC). Myosin II molecules polymerize into filaments through association of their tails, forming a compact backbone, with the heads on its surface.

For cells to conserve energy when contractile activity is not needed (e.g., muscle relaxation; nonmigrating, nondividing cells), myosin's ATPase activity and actin-binding capability are switched off. In relaxed muscle, myosin heads lie close to the thick filament backbone, away from the thin filaments, minimizing their interaction with actin and their turnover of ATP (2–4). In nonmuscle cells, myosin II in its inhibited state (low ATPase activity and actin-binding capability) exists as an inactive storage molecule (5). When contractile activity of muscle or nonmuscle cells is required, myosin activity is switched on, or enhanced, by phosphorylation of the RLCs (in nonmuscle cells and most muscles) or by Ca^{2+} binding to the ELCs (in some invertebrate muscles) (1).

The inhibited state of myosin is a key element of the energy balance of muscle cells, where myosin is the major protein. The structural basis of inhibition has been studied in vertebrate smooth and nonmuscle myosin II molecules by EM. In the inhibited state (occurring at physiological ionic strength in the presence of MgATP), myosin filaments disassemble into monomers or small oligomers (6, 7) in which the tail folds into three segments and the heads bend back and interact with each other

Significance

All animals have the ability to move. Myosin II is the motor protein that generates this movement by powering muscular contraction; it also drives motility in nonmuscle cells. In relaxed muscle and in quiescent nonmuscle cells, myosin II is switched off by intramolecular interactions between its heads that inhibit its activity. This interacting-heads motif (IHM) is a fundamental contributor to contractile regulation. Given its importance in cell contractility, we wanted to determine when the IHM first evolved. Using electron microscopy, image averaging, and sequence analysis of myosin II from primitive organisms, we show that the IHM has existed since the earliest animals and before. This ancient origin highlights the central role of the IHM in regulating myosin II function.

and with the folded tail (Fig. 1) (8–13). The activity of the heads is highly inhibited (14), apparently through these intramolecular interactions in which one head (blocked) is prevented from binding to actin through its interaction with the other head (free); the free head, in turn, has its ATPase activity inhibited by binding to the blocked head (10). When myosin is polymerized into thick filaments, as in muscle, the tails are not folded but remain extended, as required for filament formation (15). However, the heads on the filament surface undergo head–head interactions similar to those in single molecules, which, along with interactions with other heads and with the filament backbone, would also be expected to inhibit head activity (2, 16, 17). In single molecules and in most filaments a key component of this inhibited interacting-heads motif (IHM) is interaction between the proximal part of the myosin tail (referred to as "subfragment 2"; S2) and the blocked head (Fig. 1). The interactions that underlie the IHM are thought to be relatively weak (17, 18); thus the IHM reflects the average position of heads in a dynamic structure. It has been suggested that these head–head and head–tail interactions may be the basis of the super-relaxed (SRX) state of myosin (19), which has been proposed as a specific energy-conserving conformation in skeletal and cardiac muscle (20).

Interaction between heads in the inhibited state was first observed by cryo-EM of 2D crystals of vertebrate smooth muscle myosin and heavy meromyosin (a two-headed proteolytic fragment of myosin II) in the off state (10, 21). These observations were supported and further elaborated by negative-stain EM and image averaging of single smooth muscle myosin molecules (11). The latter approach had the advantage that the myosin tail and its interactions with the heads could be followed, which had not been possible in crystals. Cryo-EM 3D reconstructions of native thick filaments from invertebrate (tarantula) striated muscle demonstrated that the IHM also occurred in intact filaments in the relaxed state (2, 16, 22). The evolutionary gulf between vertebrate smooth muscle and invertebrate striated muscle suggested that the IHM must be highly conserved and that it was likely to be the basis of the relaxed state of myosin II filaments across most animal species (16).
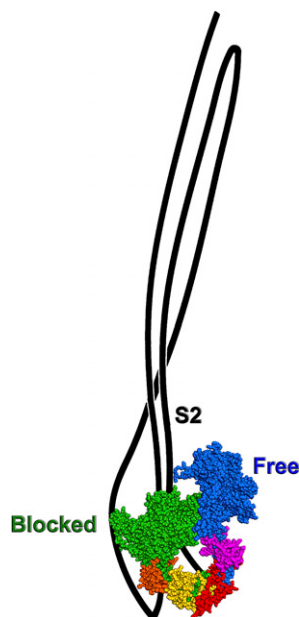

Fig. 1. The myosin II IHM in smooth muscle myosin. In the inhibited state, the tail folds into three segments, and the heads bend back onto the tail; the blocked head motor domain (green) interacts with the free head motor domain (blue) and its ELC (pink) and with all three segments of the tail, including S2. Blocked-head ELC and blocked and free RLCs are orange, yellow, and red respectively.

This view was supported by EM reconstructions of additional thick filaments regulated or modulated by RLC phosphorylation in skeletal muscle [horseshoe crab (23), scorpion (24)], smooth muscle [schistosome (25)], and cardiac muscle [mouse (26), fish (27), human (28)] or regulated by Ca^{2+} binding in striated muscle [scallop (17)]. All showed the IHM. Negative-stain EM studies of single myosin molecules from different species further supported the widespread occurrence of the IHM. Phosphorylation-regulated/modulated myosins from horseshoe crab and tarantula skeletal muscle and from vertebrate skeletal, cardiac, and nonmuscle cells (29) and Ca^{2+}-regulated myosin from molluscan striated muscle (12, 30) also all showed the IHM. Together, these results demonstrated the widespread use of the IHM as a means of switching off myosin II activity in striated muscle, smooth muscle, and nonmuscle cells. In cases when results have been obtained from single molecules and native filaments in the same system (tarantula, scallop, mouse cardiac), the motif appears similar in both, suggesting that its existence in single molecules is a reliable indicator of its likely presence in native filaments and its functioning there as a regulatory mechanism (12, 16, 17, 23, 26, 29).

The presence of the IHM in both vertebrates and invertebrates suggests that it evolved before these groups diverged. It has thus been fundamental to the control of animal movement through much of animal evolution—for at least 600 My (12). Here we look back further in evolution to ask how early this regulatory motif arose. We use EM and 2D image averaging to examine the structure of myosin II molecules in two primitive animals: sea anemones, members of *Cnidaria*, which also include jellyfish and corals and are the earliest animals with muscles, and sea sponges (*Porifera*), commonly regarded as the most primitive animals on the evolutionary tree and entirely lacking muscle tissue (31). We compare these myosins with those from unicellular organisms that predate animals and have different myosin-regulatory mechanisms (amoebozoa, fungi), and we relate the structural results to the sequences of the myosin II heavy chains (MHCs) of each species. We conclude that the IHM has been used as a means of inhibiting myosin activity since before the origin of muscle in animals and indeed before the evolution of animals themselves.

Results

We examined the structure of a variety of evolutionarily primitive myosin II molecules by EM to determine whether they exhibited the IHM in the inhibited off state. The species were chosen to include unicellular organisms [amoeba (*Acanthamoeba castellanii*), social amoeba (*Dictyostelium discoideum*), and fungus (*Schizosaccharomyces pombe*)]; primitive animals without muscle [sponge (*Cinachyra alloclada*)], and primitive animals with muscle [sea anemone (*Condylactis gigantea*)]. We used both negative staining and rotary shadowing to contrast specimens for EM. Negative staining provided greater detail, but single molecules were sometimes difficult to image; rotary shadowing gave clearer contrast but at the expense of detailed fine structure. In each case, we first examined molecules at high ionic strength in the absence of ATP (0.5 M NaAc, 1 mM EGTA, 2 mM $MgCl_2$, 10 mM Mops, pH 7.5; henceforth "high salt") to reveal their overall structure under conditions where intramolecular interactions and potential tail folding are eliminated (i.e., the off-state structure is abolished). We then observed molecules at close to physiological ionic strength (0.15 M NaAc, 1 mM EGTA, 2 mM $MgCl_2$, 10 mM Mops, pH 7.5; henceforth "low salt"), in the presence of 0.5 mM MgATP, conditions required for the off state of animal myosin II (11, 29). Most of our observations were of molecules cross-linked with glutaraldehyde (Figs. 2–7). Cross-linking stabilizes labile molecular structures (produced by weak intramolecular interactions), which can otherwise be easily disrupted by binding to the UV-treated carbon surface used with negative staining (29, 32) and to the charged mica surface used for rotary shadowing (33, 34). Cross-linked molecules were

compared with those not treated with glutaraldehyde (Fig. S1) to confirm that cross-linking had not induced a new conformation but simply helped stabilize the predominant structure already present, as found previously (35).

Vertebrate Myosin II: Smooth Muscle Myosin. As a control, we first examined the structure of vertebrate smooth muscle (turkey gizzard) myosin, which forms a stable IHM (10, 11, 21). At high ionic strength, the molecule had an extended tail, ~155 ± 2 nm in length, with two clearly resolved, flexibly attached heads which showed no tendency to interact with each other. This appearance was observed by both negative staining and rotary shadowing (Figs. 2 A and B and 3A). At low salt (150 mM; see *Methods*) in the presence of MgATP, the myosin tail appeared thicker and was approximately one-third of its length in high salt, while the heads formed a compact structure at one end of the thickened tail (Figs. 2 C and D and 3B). The thickening and shortening of the tail are consistent with its folding into thirds, as previously described for inhibited myosin II molecules (8, 9, 11, 36). The compact head structure had a triangular shape, with the apex of the triangle at the tip of the molecule. While it was difficult to distinguish the arrangement of the individual heads forming the compact structure in shadowed specimens (Fig. 2C), in negative stain (Fig. 2D) it was clear that this was generated by the contact between motor domains at the base of the triangle that was previously described (10, 11) and which is the basis of the IHM for smooth muscle myosin. A high proportion (>90%) of both cross-linked and non–cross-linked molecules showed the folded, interacting-heads structure (Fig. 2 C and D and Fig. S1A), although in the absence of cross-linking (Fig. S1A) the tail segments were often not so closely apposed to each other (9, 35).

The IHM structure in negative-stain images was revealed in greater detail by grouping molecules with similar appearances into classes and averaging the images in each class (11, 37). The class averages clearly showed the overall shape of the blocked and free heads and the contact between the two motor domains (compare Fig. 3B and Fig. S2 with Fig. 1). The three apposed segments of the folded tail, unresolved from each other, extended up from the blocked head, while a characteristic feature, representing the second fold of the tail, between its second and third segments (Fig. 1) (11, 12, 29, 35, 38), projected down from this head (arrow in Fig. 3B).

Invertebrate Myosin II: Insect Myosin. Our previous studies demonstrated the presence of the IHM in a variety of invertebrates, including arthropods. However, we had not previously studied myosin from the arthropod class Insecta, which potentially has unusual properties. With insects, the MHC is expressed in multiple isoforms that typically arise from alternative splicing of transcripts from a single gene (39). Such isoforms can show diverse functional properties that serve the requirements of the relatively slow movements of the exoskeleton (e.g., skeletal muscle of the embryonic body wall; the EMB isoform) and the rapid, oscillatory movements of the wings (indirect flight muscle; the IFM isoform) (40). We used EM to determine whether these different requirements were reflected in different structures of these two myosin isoforms from *Drosophila melanogaster*. At high salt, both myosins showed the typical extended tail lengths (tail lengths: IFM 151 ± 4 nm; EMB, 159 ± 2 nm) and flexibly attached, independently mobile heads (Fig. 4 A–D). The tail lengths are consistent with previous measurements and sequence analysis (41, 42). In low salt/MgATP, both myosins showed tail folding into three segments in almost all molecules (Fig. 4 E–H and Fig. S1 E and F), but they differed in the interaction of their heads. The EMB myosin had an IHM structure similar to that seen with smooth muscle myosin, with the heads folded back and interacting in almost all molecules (Figs. 3C and 4 G and H and Fig. S2D). In contrast, IFM molecules had more flexibly attached heads: While some exhibited head interactions similar to those in EMB (Fig. 3D and Fig. S2E), many had heads that were separated from each other and oriented at varying angles (Fig. 4 E and F). The folded tail in the vicinity of the blocked head was also less well defined for IFM averages compared with EMB, suggesting that it was more flexible in IFM (Fig. 3 C and D and Fig. S2E). We conclude that the IHM is present in both isoforms of insect myosin II but is less stable in the flight muscle.

Primitive Animal Myosin II.

Cnidaria myosin. Myosin II from sea anemone (*C. gigantea*) was examined as a representative of *Cnidaria*, the most primitive animals with muscle tissue (43), which exists as a single layer of surface cells [either smooth or striated (44)] and is used for motion of the tentacles and body. At high salt, the molecules had an appearance similar to vertebrate smooth muscle myosin: an extended tail 156 ± 5 nm in length and two flexibly attached heads clearly separated from each other and showing no tendency to interact (Fig. 5 A and C). This appearance is similar to that in a previous study of sea anemone myosin at high salt (45). At low salt, in the presence of MgATP, the molecules adopted a compact structure (Fig. 5 B and D) similar to that of vertebrate smooth muscle myosin (Fig. 2 C and D), showing that *Cnidaria* myosin also forms an IHM structure. This was confirmed in image averages (Fig. 3E and Fig. S2B). The appearance was similar without cross-linking (Fig. S1B), although the non–cross-linked molecules often had a looser structure. We conclude that the IHM is present in the most primitive animals with muscles.

Porifera myosin. We next studied myosin II from the Demosponge *C. alloclada* as a representative of *Porifera* (sponges), commonly regarded as the earliest animal phylum on the evolutionary tree (46, 47). While sponges are multicellular organisms, they lack discrete muscle tissue, although they do possess individual "myocytes" that resemble smooth muscle cells (31). These contain thick and thin filaments and are thought to function in closing the osculum used for water expulsion (48, 49). Because of
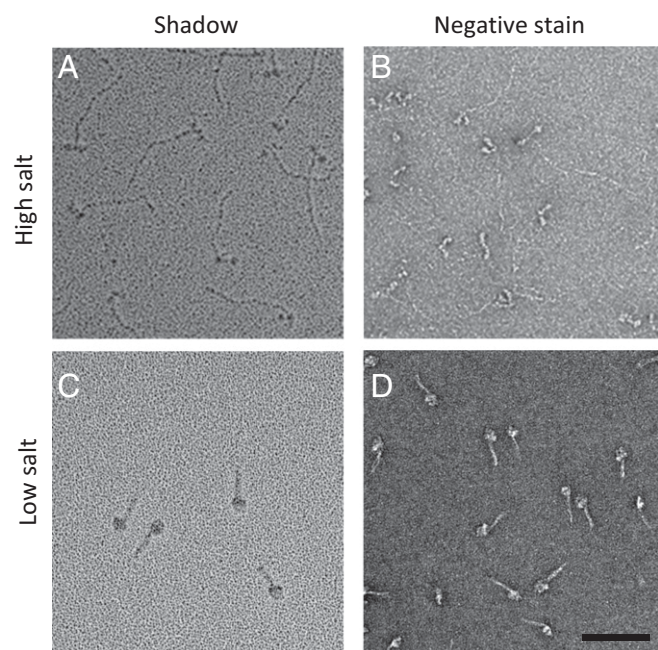

Fig. 2. Vertebrate smooth muscle myosin molecules. Molecules were imaged by rotary shadowing (A and C) or negative staining (B and D) under high-salt (A and B; extended molecules) or low-salt/MgATP (C and D; folded molecules with interacting heads) conditions. (Scale bar: 100 nm.)
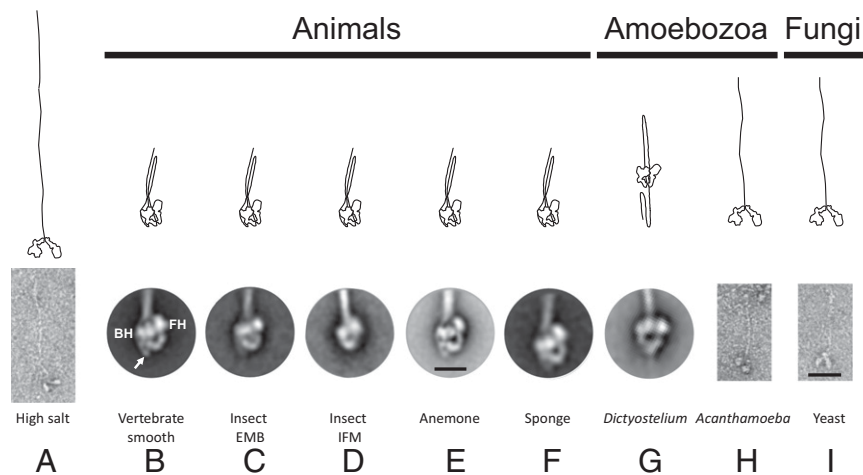
Lee et al.

Fig. 3. Conformations of different myosin II molecules. Cartoons (approximately to scale) show folded or extended tail accompanied respectively by folding back and interaction of heads with each other and with the tail or the absence of these interactions. Below the cartoons are class averages of folded molecules and single images of unfolded molecules (averaging was not possible due to the varied conformation of these molecules). (*A*) In high salt, all the myosins had an extended tail and noninteracting heads; sponge myosin is shown as an example. (*B–I*) In low salt/MgATP, most myosins show an IHM (*B–G*), but *Acanthamoeba* and fission yeast do not (*H* and *I*). Folding of the lower half of the tail in *Dictyostelium* is variable and difficult to define, due to the close apposition of the segments. The cartoon shows one likely arrangement based on an analysis of the lengths of the tail regions projecting on the two sides of the heads. BH, blocked head; FH, free head; arrow shows second fold in tail. Scale bars: *A*, *H*, and *I*, 50 nm; *B–G*, 15 nm.

the small quantities of myosin obtained from the sponge, we used only negative staining for EM observation, as this requires less protein than rotary shadowing. At high salt, sponge myosin had an extended structure (tail length 155 ± 4 nm) with flexibly attached, noninteracting heads (Fig. 5*E*), similar to vertebrate smooth and *Cnidarian* myosin and to the morphology seen in an earlier study (50). In low salt, containing MgATP, the tails again folded into three segments, and the heads pointed back, showing clear head–head interactions in both single molecules and class averages (Figs. 3*F* and 5*F* and Fig. S2*C*), similar to vertebrate smooth and *Cnidarian* myosin. We conclude that the IHM is present in the most primitive of all animals on the evolutionary tree.

Myosin II in Unicellular Organisms. To determine whether the IHM was present in unicellular organisms that predate animals, we studied myosin II in amoebozoa and fungi (51).

Acanthamoeba myosin. In *A. castellanii*, myosin II is used for locomotion and cell division (52) but is regulated by a different mechanism from animal myosin IIs: Phosphorylation of the nonhelical tip of the tail hinders its assembly into filaments (53), while phosphorylation of the motor domain heavy chain inhibits actin activation of its myosin ATPase (54, 55). We used an expressed myosin in which the motor domain and tip of the tail contained phosphomimetic mutations (53, 54) to simulate the inhibited state. At high salt, this myosin had an extended tail and no signs of head–head interaction, as with the animal myosin IIs (Fig. 6 *A* and *B*). However, the tail was much shorter than that of animal myosins (87 ± 8 nm compared with ~155 nm), as found previously (53, 56) and consistent with the shorter α-helical coiled-coil sequence of *Acanthamoeba* myosin compared with animal myosin IIs (57). In low salt/MgATP, the structure looked identical to that in high salt (Figs. 3*H* and 6 *E* and *F*). The tail remained fully extended, with no sign of the folding seen in all of the animal myosin IIs, and the heads remained separate and flexibly attached to the tail, with no indication of intramolecular interaction. This result was also found in molecules that were not cross-linked (Fig. S1*C*). We conclude that the structural mechanism for switching off myosin II activity in amoebae is different from that in animals and does not rely on interacting heads.

Yeast myosin. Yeasts are ancient, single-celled eukaryotes that are part of the fungus kingdom and are thought to have arisen about 1,000 Mya (58, 59). Two myosin IIs are expressed in the fission yeast *S. pombe* (60). Myo2 is known to function in cytokinesis, but its mechanism of regulation is not yet understood. Myo2 at high salt had an appearance similar to the other myosins described above, with an extended tail and flexibly attached heads (Fig. 6 *C* and *D*). As with *Acanthamoeba*, however, the tail was

shorter (91 ± 4 nm) than that of the animal myosins, consistent with previous measurements and with the length of the coiled-coil sequence in this myosin (61). Under conditions that produce the compact, inhibited state of animal myosin II (low salt and MgATP), Myo2 showed the same structure as in high salt (Figs. 3*I* and 6 *G* and *H*): The tail remained extended, and the heads showed multiple orientations, with no tendency to interact with each other. This is similar to the result with *Acanthamoeba* myosin II and is quite distinct from the behavior of animal myosins.

Social amoeba myosin. Slime molds are unicellular amoebozoan eukaryotes that predate animals (62). In addition to living as single cells, "cellular" slime molds (or social amoebae, e.g., *D. discoideum*) can also form multicellular aggregates when food is in short supply. *Dictyostelium* myosin II functions in cortical rigidity, cell growth, and cytokinesis (63–65). The regulation of *Dictyostelium* myosin II has features in common with both animal and *Acanthamoeba* myosins. While heavy-chain phosphorylation in the C-terminal third of the α-helical tail promotes disassembly

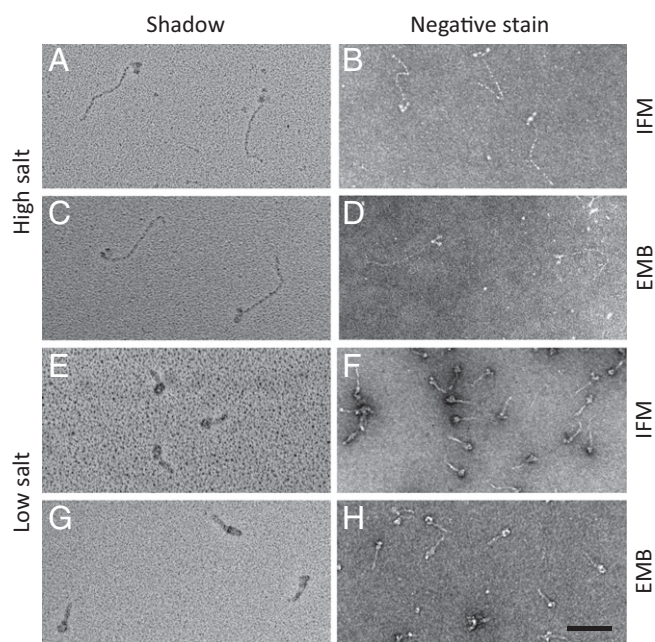

Fig. 4. Insect muscle myosin II molecules. IFM and EMB myosin under high-salt (*A–D*; extended molecules) or low-salt/MgATP (*E–H*; folded molecules) conditions were imaged by rotary shadowing or negative staining. (Scale bar: 100 nm.)
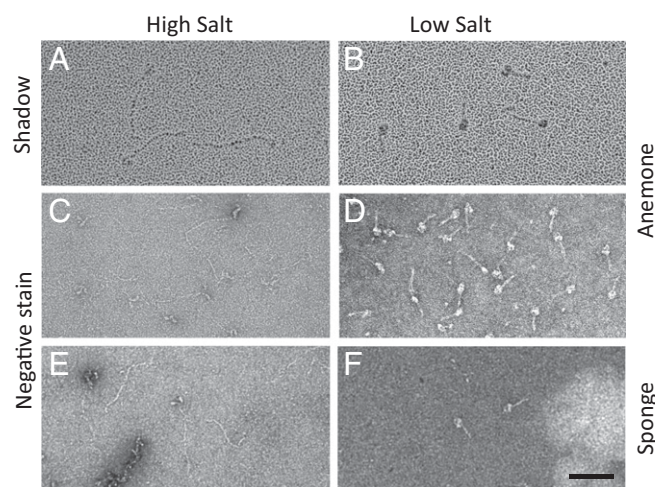
Fig. 5. Sea anemone and sponge myosin II molecules. Myosin under high-salt (A, C, and E; extended molecules) or low-salt/MgATP (B, D, and F; folded molecules) conditions was imaged by rotary shadowing or negative staining. (Scale bar: 100 nm.)

of filaments (similar to phosphorylation of the nonhelical tip of the *Acanthamoeba* myosin tail), interaction with actin is favored by phosphorylation of the RLC, similar to animal myosin IIs (although this activation effect is smaller than with animal myosins) (66, 67). *Dictyostelium* myosin with a phosphorylated tail and unphosphorylated RLC (conditions favoring inhibition of enzymatic activity and filament assembly) was examined by EM. At high salt, the molecules showed the usual extended tail with flexibly attached heads (Fig. 7 A and B), but the tail (185 ± 3 nm) (68) was about twice as long as in fission yeast and *Acanthamoeba* myosin and was ∼20% longer than in animal myosin. When incubated at low salt in the presence of MgATP, the myosin heads frequently appeared to interact with each other in a manner resembling, but not identical to, that in the animal myosins (Figs. 3G and 7 C and D and Fig. S2F). The tail was also folded, but the folding was different from the animal myosins. The first bend was in a similar position to these myosins, but the tail then passed the heads and folded again one or more times on the other side of the heads (Fig. 3G). A similar appearance was seen both with (Fig. 7 C and D) and without (Fig. S1D) cross-linking. This suggests that a form of head–head interaction had already evolved before the origin of animals.

Relation of the MHC Sequence to the IHM. The complete MHC sequences of the species studied by EM were aligned with other MHC sequences to compare their homology. The average distance tree of these sequences split into two main branches: a striated muscle-like branch and a smooth/nonmuscle-like branch (Fig. 8). The striated-like branch included sequences of both vertebrate and invertebrate striated MHCs. The smooth/nonmuscle-like branch included the smooth and nonmuscle-like sequences of vertebrates and the nonmuscle-like sequences of invertebrates and primitive unicellular organisms (amoebozoa and fungi). Within the smooth/nonmuscle branch, the amoebozoa and fungi sequences were distinct from the animal sequences (69). A previous analysis of MHC sequences showed strong association between the presence of the IHM and a conservation score of >63% of the interactions thought to be involved in creating its intramolecular interfaces (70). For the species studied here, conservation scores ranged from 72% and 79% (*Drosophila* EMB and IFM MHCs) and 63–75% for sponge to only 29–32% for amoebozoa (*Acanthamoeba* and *Dictyostelium*) (70). Thus, the amino acids involved in the intramolecular interactions of

the IHM from striated, smooth, and nonmuscle cells of animals are more conserved (≥63%) than those from amoebozoa (≤32%).

Discussion

Myosin II appears to have arisen early in the evolution of eukaryotes and then diverged into striated-like and smooth-like classes (Fig. 8) (71, 72). All three classes exhibit the IHM in all metazoa previously studied (10–12, 16, 17, 23–29), dating back as far as arthropods, mollusks, and flatworms—at least 600 My (12, 17, 25). Here we demonstrate that the IHM is even older, present in both *Cnidaria* (the most primitive animals with muscles) and *Porifera* [usually considered the earliest animal phylum (73), possessing myocytes but lacking muscle and other tissues], which may have emerged up to 700 and 900 Mya, respectively (74–76). The IHM in all these animals appears essentially identical to that in vertebrate smooth muscle myosin, which we used as a control (Figs. 2, 3, and 5). This correlates with high charge conservation of the amino acids thought to be involved in the sites of electrostatic interaction within the intramolecular interfaces of the IHM in different species (70). Surprisingly, we also found what appeared to be a modified version of the IHM in one of the eukaryotes that predate animals (*Dictyostelium*) (Figs. 3 and 7). This structural conservation suggests that head–head interaction has played a central role in regulating muscle contraction and cell motility from the earliest metazoans and before.

Significance of the IHM in Thick Filaments. The physiological role of the IHM in thick filaments is demonstrated in studies of vertebrate striated muscle. X-ray diffraction and fluorescence polarization observations reveal that in relaxed muscle, myosin heads lie in pseudohelical arrays on the filament surface (3, 77), in the IHM configuration (78, 79), in agreement with EM studies of isolated filaments (16, 17, 23–28). Surprisingly, x-ray data show that even during contraction (under low load), most heads lie on the filament surface in their relaxed, helically ordered IHM
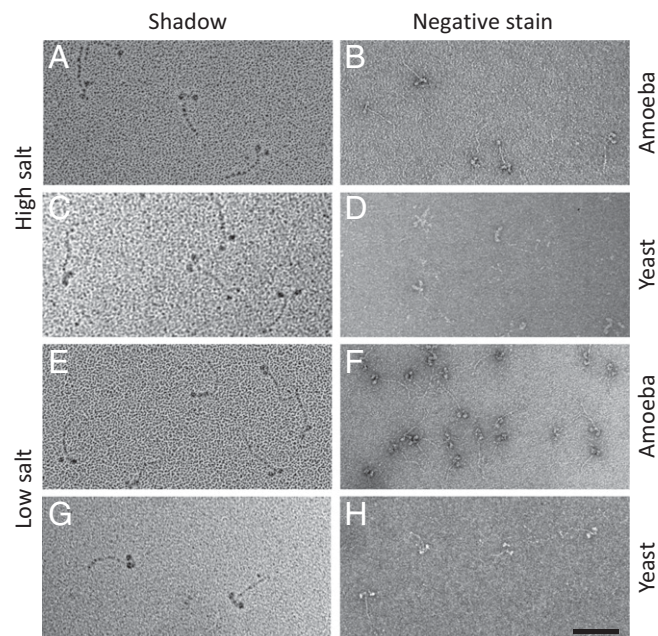

Fig. 6. *Acanthamoeba* and yeast (*S. pombe*) myosin II molecules. Myosin under high-salt (A–D) or low-salt/MgATP (E–H) conditions was imaged by rotary shadowing or negative staining. In all cases molecules were extended (but with a shorter tail than in the animal and *Dictyostelium* myosin), and there was no sign of head–head interaction. (Scale bar: 100 nm.)
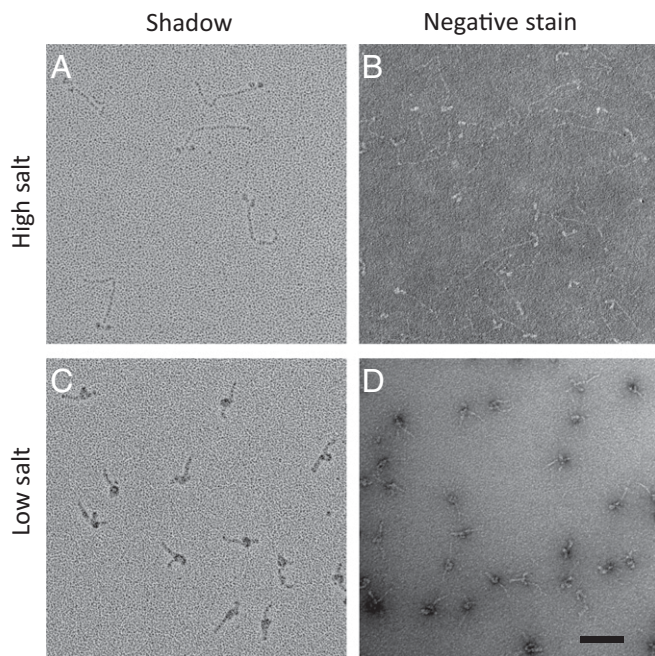
Fig. 7. *D. discoideum* myosin II molecules. Myosin under high-salt (*A* and *B*; extended molecules) or low-salt/MgATP (*C* and *D*; folded molecules) conditions was imaged by rotary shadowing or negative staining. Molecules had a longer tail than the animal, amoeba, and yeast myosins, and part of the tail extended in the opposite direction to the folded heads (see Fig. 3*G*). (Scale bar: 100 nm.)

arrays, with only a small fraction interacting with actin (80). Thus, the IHM plays a central role in contraction as well as relaxation. When muscle contracts isometrically, placing tension on the thick filaments, all heads leave their ordered IHM arrays, making them available to interact with actin (3, 80). When stimulation ceases, helically ordered heads are reestablished within 20 ms, suggesting that re-formation of the IHM is an integral feature of relaxation (80, 81). Time-resolved EM studies of thick filaments confirm the rapid reformation of helically ordered IHMs on relaxation (82). When a sudden step shortening is imposed during isometric contraction (heads fully disordered), allowing transient isotonic shortening, helically ordered IHMs are again reestablished within 20 ms (80). These physiological findings, together with the evolutionary conservation of the IHM, lead to the same conclusion: The IHM is an integral component of muscle relaxation and low-load contraction. It is the default configuration of myosin heads. The significance of the IHM to muscle function is further suggested by the finding that myosin mutations causing hypertrophic cardiomyopathy in humans are concentrated largely at the sites of interaction that generate the IHM (83, 84). The locations of many of these mutations predict impaired IHM stability, which could account for the altered systolic and diastolic function (83, 84) and increased energy consumption that characterize hypertrophic cardiomyopathy (83). Thus, a compromised IHM structure can lead to severe and sometimes lethal cardiac disease (83).

Significance of the IHM in Single Myosin II Molecules. While the function of the IHM in muscle thick filaments is clear, its role in single myosin II molecules is less so. In nonmuscle cells, the folding of the tail and interaction of the heads produces a molecule with low ATPase activity and inhibited actin binding. This inactive form is thought to be stored, ready for use, as monomers or small oligomers (6, 7) that consume little cellular energy (5). When motility is needed, the compact structure of the folded monomer or oligomers would facilitate their transport to the

required cellular location, where RLC phosphorylation promotes unfolding and assembly into active filaments that can interact with actin (6, 7, 9, 85, 86).

Does the folded single-molecule conformation also have a role in muscle cells (11, 12, 29)? In vertebrate smooth muscle, myosin filaments can be permanent structures (87, 88), or they can be more labile, increasing their length or number upon activation, probably through RLC phosphorylation-based augmentation from a pool of myosin monomers or small oligomers, similar to nonmuscle cells (89–91). Here the folded form of smooth muscle myosin may also function as a storage molecule (92). In striated muscle, myosin II is assumed to exist as permanent filaments: Are folded, soluble molecules also present? The existence of a significant (40-nM) critical concentration of myosin in equilibrium with filaments suggests that they are (93–95). The folded monomer could play a crucial role in the assembly and turnover of filaments that occur in normal striated muscle development, maintenance, growth, and repair (96). Following synthesis, polypeptide chains detach from ribosomes and assemble into mature molecules (in the case of myosin II, containing two heavy chains and four light chains). If their local concentration is low, these myosin molecules could fold into the inhibited structure that we observe, without forming filaments, as they do in our in vitro experiments. This folded structure could act as a transport form of myosin, whose compact configuration facilitates both its movement (e.g., through the filament lattice) to the site of filament assembly and the prevention of premature filament formation on its way (96). On reaching the site of assembly, molecules could be triggered to unfold and incorporate into nascent filaments, e.g., by interaction with titin or myosin tails on the filament surface. Myosin chaperones may also play a role in this process (97, 98). This model would be analogous to the synthesis of collagen inside fibroblasts, where intracellular assembly of procollagen molecules into fibrils is prevented by the presence of bulky peptides at the molecular ends. Upon secretion, these peptides are cleaved off, and the mature collagen molecules self-assemble into fibrils in the extracellular space (99, 100). If this speculation is correct, it could explain why striated as well as smooth muscle and nonmuscle myosin II has retained the ability to form an inactive, compact conformation, since striated muscles first evolved.

Presence of the IHM in Insects. While the IHM appears to be ubiquitous through most of the animal kingdom, we reasoned that there might be exceptions, for example in muscles where the relaxed state is very short-lived. The most obvious instance is insect IFM, in which contraction–relaxation cycles can occur hundreds of times per second (101). A recent cryo-EM 3D reconstruction of insect IFM thick filaments supports this view (102). While an IHM is present, it has a modified form: The two heads interact through their motor domains as in the IHMs of other animal thick filaments, but the motif is rotated by 90°, so that it is perpendicular to the thick filament axis, and it is the free rather than the blocked head that is the more constrained. Significantly, unlike other animals, there also appears to be no interaction between S2 and the blocked head (102). To understand this further, we compared the structures of *Drosophila* EMB and IFM myosin molecules (40). The EMB molecule (which functions in conventional, relatively slow movements of the larval exoskeleton) showed the normal IHM structure seen in the other animal myosins. While some IFM molecules showed similar head interactions, many had heads that were much more flexibly attached, and the tail in the vicinity of the heads was less clearly defined (Fig. 3*D* and Fig. S2*E*). This could relate to the absence of the S2-blocked head interaction in the filaments (102), which in turn is explicable by the loss of negative charge in S2 (compared with other species) in its region of contact with the blocked head (103). With fewer interaction sites, the IHM in
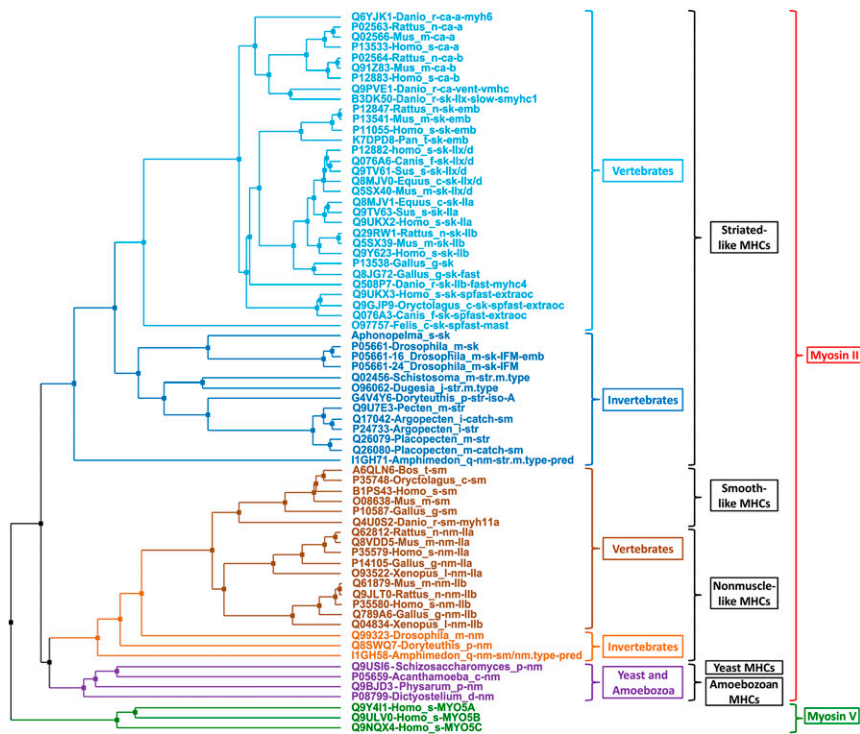
www.manaraa.com

Fig. 8. Average distance tree for MHCs from sequence alignment. The MHC sequences segregate into two major groups according to their MHC type [a similar segregation is obtained by comparing ELC and RLC sequences (72)]: (*i*) striated-like MHCs in vertebrates (cyan) and invertebrates (blue); (*ii*) smooth/nonmuscle-like MHCs in vertebrates (brown), invertebrates (orange), and amoebozoa and fungi (purple). Within the smooth/nonmuscle-like group, amoebozoa and fungi were distinct from animals. The bottom group in green (myosin V isoforms) is shown for comparison, as myosin V does not establish IHMs. The horizontal axis reflects sequence similarity (horizontal lines are shorter for more similar sequences), not evolutionary divergence times. The latter have been estimated for Amoebozoa, fungi, and Metazoa as 1,425–1,675, 975–1,225, and 725–850 Mya, based on the time-calibrated tree of ref. 59.

insect flight muscle may be able to form and break more rapidly, consistent with the rapid wing beat. This also correlates with the increased ATPase rate for the IFM isoform (40). We conclude that the IHM is present in both isoforms of insect myosin II but is less stable in the flight muscle, presumably as a result of differences in critical regions of the protein that are encoded by alternative exons (40, 103). This is consistent with the lower level of charge attraction predicted (on the basis of sequence comparison) in the IHM interfaces of IFM compared with EMB myosin (70, 103).

The IHM in Unicellular Animals. The amoeboid unicellular organisms *A. castellanii* and *D. discoideum*, evolved before the advent of animals. While myosin II molecules in these organisms are known to be regulated by phosphorylation, the kinases and the sites and effects of phosphorylation are different from those in animal myosin II (53–55, 67). We therefore expected that the structural mechanism of regulation, and in particular the inhibited state, might be different. This was confirmed in the case of *Acanthamoeba*, where inhibited molecules (with phosphorylated tail and head) examined under relaxing conditions (the same low salt/MgATP conditions we used for muscle myosins) showed no sign of the head–head or head–tail interactions that switch off activity in animal myosin II (Fig. 6). However, our observation of a modified version of the IHM in *Dictyostelium* (Fig. 7) suggests that a form of IHM may already have evolved before multicellular animals arose. *Dictyostelium* is a social amoeba, a class of organisms that normally exist as single cells but under starvation conditions form multicellular fruiting bodies (104). It is interesting that, of the three unicellular organisms that we studied, the only one that shows head–head interactions is also the only one that can exist in a multicellular form, one of the defining features of animals. Control of the actin-activated ATPase of *Dictyostelium* myosin II is also similar to that of animal myosin II, occurring through RLC phosphorylation (105). This suggests that the IHM/RLC phosphorylation mechanism for regulating myosin II may possess evolutionary advantages for multicellular organisms and sup-

ports other findings of similarities between social amoebae and metazoa (104, 106).

While we conclude that the modified form of IHM we observe in *Dictyostelium* is likely to represent an inhibited state (as in animals), which is maintained in the filamentous form, our results do not shed light on the structural mechanism of inhibition in *Acanthamoeba* or yeast myosin II, neither of which shows a distinctive inhibited conformation. Phosphorylation of the tip of the tail of *Acanthamoeba* myosin II inhibits dimerization and reduces filament size (53). Our results show that inhibition of assembly is not due to tail folding as in the other myosin IIs; it may occur instead through charge repulsion (53). Actin-activated *Acanthamoeba* myosin ATPase is inhibited by phosphorylation of the motor domain at residue 639 of the heavy chain (53). The structural basis of this inhibition remains unknown, but our results show that it does not involve the head interactions seen in the IHM. Interestingly, yeast myosin II also shows no tendency for tail folding or head–head interactions; its mechanism of regulation has yet to be determined (107). Both fission yeast and *Acanthamoeba* myosin IIs have much shorter tails (~87–91 nm) than animal (~155 nm) and *Dictyostelium* (185 nm) myosin IIs; thus, some of the head–tail interactions that stabilize the IHM in the latter myosins are not possible in the former, possibly contributing to the absence of the folded structure.

Relation of MHC Sequence to the IHM. Sequence alignment (Fig. 8) provides important insights into the correlation between MHC type (striated, smooth, or nonmuscle-like) and the presence of the IHM (70). It is clear that all three types of myosin II can fold into the inhibited IHM structure (Figs. 3 and 8) (29). The IHM thus underlies the switched-off state of myosin filaments in muscle and of myosin molecules in nonmuscle and muscle cells, as discussed above. Our results suggest that the IHM structure may have been a feature of the original MHC thought to have given rise to subsequent striated and smooth/nonmuscle isoforms by gene duplication (69), and that the motif may have persisted throughout the process that subsequently led to distinct smooth and striated muscle cell types (108). The IHM has been found in

Lee et al.

all animals in which it has been sought, correlating with conservation of proposed interacting residues in these animals (70); the absence of the IHM from amoeba (*A. castellanii*) and yeast (*S. pombe*) correlates with poor conservation of these residues (70). The presence of an IHM in the social amoeba, *Dictyostelium*, was not expected, based on similarly poor conservation in this species (70). Its existence, together with its modified form compared with the animal IHMs, suggests that it may have evolved independently in *Dictyostelium* (raising the possibility that other modified versions of the IHM may exist in ancestors of animals that have not yet been studied). Alternatively, myosin II in the common ancestor of amoebozoans, fungi, and metazoans (69, 109) may already have evolved an IHM-like structure, which was then lost in some amoebozoa (e.g., *A. castellanii*) and fungi (e.g., *S. pombe*) but was retained in metazoans and in *Dictyostelium* (in modified form). Within the animal kingdom, the structure of the IHM is well conserved, although variations may occur in specialized situations, such as insect flight muscle (102).

The SRX State and the IHM. A substantial portion of myosin heads in the thick filaments of relaxed muscle have been shown to occur in an energy-saving state (the SRX state), in which ATP turnover is highly inhibited (19, 20). The SRX state is found in vertebrates and invertebrates and in both cardiac and skeletal muscles (19, 20, 110, 111). A strong correlation between the presence of the SRX state in muscle and the IHM structure in thick filaments suggests that the IHM is the structural basis of this inhibited state (20, 70). The head–head and head–tail interactions that characterize single myosin molecules from vertebrate smooth and invertebrate striated muscles also lead to highly inhibited ATPase activities (14, 96), befitting their storage function (5). Our structural findings, showing IHMs as far back as the earliest animals (*Porifera*) and apparently even before (*Dictyostelium*), support the proposal that this mechanism of ATP conservation arose very early in the evolution of myosin II molecules (70).

Many enzymes are regulated by self-inhibitory mechanisms (112, 113) in which the inhibited form is generally a compact, folded structure. In the case of the myosin superfamily, at least three variations of autoinhibition exist (114). With myosin II, inhibition occurs through the asymmetric head–head and head–tail interactions that we have discussed. In contrast, myosin V does not form an IHM but is inhibited by the folding back of heads onto its tail so that its cargo-binding domain at the tip of the tail can interact with each of the heads without any interaction between the heads themselves (115–118). The single-headed myosins VIIA and X are inhibited by the folding back and interaction of their short tails with their head/neck region (119–121). In the case of microtubule-associated motors, inhibition again occurs through intramolecular interaction. Kinesins are generally inhibited by the binding of specialized regions of their tails to their motor domains, made possible through folding of the coiled-coil tail part way along its length (122). In the case of dynein, the underlying structural mechanism of inhibition is similar to myosin II: in the autoinhibited state the two motor heads are stacked one upon the other, preventing their productive interaction with microtubules (123). How did these regulatory mechanisms originate? One scenario is that motor proteins first evolved in an unregulated (always active) form and that this metabolically inefficient mechanism later became regulated. Evidence for this possibility comes from studies of the evolution of kinases using phylogenetic resurrection techniques, which suggest that ancestral kinases were unregulated and that regulatory elements appeared later in evolution (124).

Methods

Myosin II Preparation. Smooth muscle myosin II from turkey gizzard was purified according to ref. 125. Sea anemone myosin was purified from *C. gigantea* according to ref. 45 with slight modifications. The purified myosin was rapidly frozen in liquid nitrogen and stored at −80 °C. Sea sponge myosin was prepared from *C. alloclada* according to ref. 50 with modification. For both anemone and sponge preparations we added a protease inhibitor, diisopropylfluorophosphate (DFP, 0.5 mM), to the extract and 0.2 mM DFP throughout the preparation and used a BioSep SEC-s4000 (Phenomenex) for HPLC. Myosin II prepared from these species has predominantly dephosphorylated RLCs and is therefore in the off state (45, 50, 125). Recombinant *Acanthamoeba* myosin II was obtained by coexpression of N-terminal FLAG-tagged heavy chain and two light chains in Sf9 cells and was purified by FLAG-affinity chromatography (54). This enabled molecules to be engineered to mimic the off state by replacing the regulatory serines in the motor domain and the tip of the tail with aspartate (53–55). *Dictyostelium* myosin was prepared and phosphorylated as described previously (67, 126). Fission yeast (*S. pombe*) myosin (Myo2) expressed in Sf9 cells was the gift of Luther Pollard, Kathleen Trybus, and Susan Lowey, Department of Molecular Physiology and Biophysics, University of Vermont, Burlington, VT (107). *Drosophila* IFM and EMB myosins were expressed transgenically in IFMs null for endogenous myosin (127). Protein was isolated from ~200 dissected IFMs as previously detailed (128).

EM. Myosin molecules were examined under high-salt conditions (0.5 M NaAc, 1 mM EGTA, 2 mM MgCl$_2$, 10 mM Mops, pH 7.5), and in low salt in the presence of MgATP (0.15 M NaAc, 1 mM EGTA, 2.5 mM MgCl$_2$, 0.5 mM ATP, 10 mM Mops, pH 7.5). Myosin at 10 nM was negatively stained with 1% (wt/vol) uranyl acetate on carbon films pretreated with UV light to optimize stain spreading (29, 129). For rotary shadowing, myosin at 400 nM in high salt or low salt/MgATP was mixed with an equal volume of glycerol and then was sprayed onto freshly cleaved mica before shadowing with platinum at a 6° angle while rotating the specimen (9, 130). In some cases, chemical cross-linking was used to stabilize molecules against the forces of binding to the carbon or mica surface: Molecules were treated in solution at room temperature for 1 min with 0.1% glutaraldehyde before negative staining or spraying for rotary shadowing (29, 35). Images were recorded on a Philips CM120 electron microscope at 120 kV with a 2K × 2K CCD camera (F224HD, Tietz Video and Image Processing Systems, GmbH) or on a Tecnai Spirit G2 BioTWIN microscope operating at 120 kV using a Gatan Erlangshen CCD camera. Tail length measurements ± SD were made from negative-stain images (at least 40 molecules in each case) by counting pixels and multiplying by the calibrated pixel size.

Image Processing. Images of myosin II molecules were manually selected from electron micrographs using EMAN2 (131). The numbers of particles used were 8,241 (vertebrate smooth muscle), 3,552 (sea anemone), 694 (sponge), 4,912 (insect EMB), 4,327 (insect IFM), and 4,765 (*Dictyostelium*). 2D classification and class averages were carried out using RELION (132). To remove flexible or bad particles, three iterations of 2D classification were performed for each dataset. Particles giving rise to averages in which features were poorly defined were removed for subsequent iterations.

Bioinformatics. We calculated the tree in Fig. 8 (see ref. 25) by applying distance matrices determined from the percent identity of amino acid sequences using the Average Distance algorithm (UPGMA: Unweighted Pair Group Method using Arithmetic Averages) of Jalview (ver. 2.8) (133, 134). We used this average distance tree of aligned MHC sequences to classify the myosins into smooth, striated, or nonmuscle-like (25): Invertebrate myosin II molecules are either nonmuscle-like or striated-like (135), whereas vertebrate myosin II also includes a smooth-like type similar in sequence to nonmuscle myosin (136, 137). Only complete sequences (with experimental evidence at the protein and transcript level) were included in the alignment. The sequences were retrieved from UniProt (www.uniprot.org/) (133) and were aligned with MUSCLE (ver. 3.8.31) using default parameters (138).

www.manaraa.com

1. Sellers JR (1999) *Myosins* (Oxford Univ Press, New York), 2nd Ed.
2. Craig R, Woodhead JL (2006) Structure and function of myosin filaments. *Curr Opin Struct Biol* 16:204–212.
3. Huxley HE, Brown W (1967) The low-angle X-ray diagram of vertebrate striated muscle and its behaviour during contraction and rigor. *J Mol Biol* 30:383–434.
4. Huxley HE (1968) Structural difference between resting and rigor muscle; evidence from intensity changes in the low-angle equatorial X-ray diagram. *J Mol Biol* 37:507–520.
5. Cross RA (1988) What is 10S myosin for? *J Muscle Res Cell Motil* 9:108–110.
6. Kendrick-Jones J, Smith RC, Craig R, Citi S (1987) Polymerization of vertebrate non-muscle and smooth muscle myosins. *J Mol Biol* 198:241–252.
7. Liu X, et al. (2017) Effect of ATP and regulatory light-chain phosphorylation on the polymerization of mammalian nonmuscle myosin II. *Proc Natl Acad Sci USA* 114:E6516–E6525.
8. Onishi H, Wakabayashi T (1982) Electron microscopic studies of myosin molecules from chicken gizzard muscle I: The formation of the intramolecular loop in the myosin tail. *J Biochem* 92:871–879.
9. Craig R, Smith R, Kendrick-Jones J (1983) Light-chain phosphorylation controls the conformation of vertebrate non-muscle and smooth muscle myosin molecules. *Nature* 302:436–439.
10. Wendt T, Taylor D, Trybus KM, Taylor K (2001) Three-dimensional image reconstruction of dephosphorylated smooth muscle heavy meromyosin reveals asymmetry in the interaction between myosin heads and placement of subfragment 2. *Proc Natl Acad Sci USA* 98:4361–4366.
11. Burgess SA, et al. (2007) Structures of smooth muscle myosin and heavy meromyosin in the folded, shutdown state. *J Mol Biol* 372:1165–1178.
12. Jung HS, et al. (2008) Conservation of the regulated structure of folded myosin 2 in species separated by at least 600 million years of independent evolution. *Proc Natl Acad Sci USA* 105:6022–6026.
13. Lowey S, Trybus KM (2010) Common structural motifs for the regulation of divergent class II myosins. *J Biol Chem* 285:16403–16407.
14. Cross RA, Jackson AP, Citi S, Kendrick-Jones J, Bagshaw CR (1988) Active site trapping of nucleotide by smooth and non-muscle myosins. *J Mol Biol* 203:173–181.
15. Huxley HE (1963) Electron microscope studies on the structure of natural and synthetic protein filaments from striated muscle. *J Mol Biol* 7:281–308.
16. Woodhead JL, et al. (2005) Atomic model of a myosin filament in the relaxed state. *Nature* 436:1195–1199.
17. Woodhead JL, Zhao FQ, Craig R (2013) Structural basis of the relaxed state of a Ca2+-regulated myosin filament and its evolutionary implications. *Proc Natl Acad Sci USA* 110:8561–8566.
18. Sulbarán G, et al. (2013) Different head environments in tarantula thick filaments support a cooperative activation process. *Biophys J* 105:2114–2122.
19. Stewart MA, Franks-Skiba K, Chen S, Cooke R (2010) Myosin ATP turnover rate is a mechanism involved in thermogenesis in resting skeletal muscle fibers. *Proc Natl Acad Sci USA* 107:430–435.
20. Cooke R (2011) The role of the myosin ATPase activity in adaptive thermogenesis by skeletal muscle. *Biophys Rev* 3:33–45.
21. Liu J, Wendt T, Taylor D, Taylor K (2003) Refined model of the 10S conformation of smooth muscle myosin by cryo-electron microscopy 3D image reconstruction. *J Mol Biol* 329:963–972.
22. Alamo L, et al. (2008) Three-dimensional reconstruction of tarantula myosin filaments suggests how phosphorylation may regulate myosin activity. *J Mol Biol* 384:780–797.
23. Zhao FQ, Craig R, Woodhead JL (2009) Head-head interaction characterizes the relaxed state of Limulus muscle myosin filaments. *J Mol Biol* 385:423–431.
24. Pinto A, Sánchez F, Alamo L, Padrón R (2012) The myosin interacting-heads motif is present in the relaxed thick filament of the striated muscle of scorpion. *J Struct Biol* 180:469–478.
25. Sulbarán G, et al. (2015) An invertebrate smooth muscle with striated muscle myosin filaments. *Proc Natl Acad Sci USA* 112:E5660–E5668.
26. Zoghbi ME, Woodhead JL, Moss RL, Craig R (2008) Three-dimensional structure of vertebrate cardiac muscle myosin filaments. *Proc Natl Acad Sci USA* 105:2386–2390.
27. González-Solá M, Al-Khayat HA, Behra M, Kensler RW (2014) Zebrafish cardiac muscle thick filaments: Isolation technique and three-dimensional structure. *Biophys J* 106:1671–1680.
28. Al-Khayat HA, Kensler RW, Squire JM, Marston SB, Morris EP (2013) Atomic model of the human cardiac muscle myosin filament. *Proc Natl Acad Sci USA* 110:318–323.
29. Jung HS, Komatsu S, Ikebe M, Craig R (2008) Head-head and head-tail interaction: A general mechanism for switching off myosin II activity in cells. *Mol Biol Cell* 19:3234–3242.
30. Gillilan RE, Kumar VS, O'Neall-Hennessey E, Cohen C, Brown JH (2013) X-ray solution scattering of squid heavy meromyosin: Strengthening the evidence for an ancient compact off state. *PLoS One* 8:e81994.
31. Ruppert EE, Fox RS, Barnes RD (2004) *Invertebrate Zoology* (Brooks/Cole, Belmont, CA).
32. Knight P, Trinick J (1984) Structure of the myosin projections on native thick filaments from vertebrate skeletal muscle. *J Mol Biol* 177:461–482.
33. Trinick J, Elliott A (1982) Effect of substrate on freeze-dried and shadowed protein structures. *J Microsc* 126:151–156.
34. Stafford WF, et al. (2001) Calcium-dependent structural changes in scallop heavy meromyosin. *J Mol Biol* 307:137–147.
35. Jung HS, et al. (2011) Role of the tail in the regulated state of myosin 2. *J Mol Biol* 408:863–878.
36. Trybus KM, Huiatt TW, Lowey S (1982) A bent monomeric conformation of myosin from smooth muscle. *Proc Natl Acad Sci USA* 79:6151–6155.
37. Frank J (2006) *Three-Dimensional Electron Microscopy of Macromolecular Assemblies: Visualization of Biological Molecules in Their Native State* (Oxford Univ Press, New York), 2nd Ed.
38. Yang S, Lee KH, Sato O, Ikebe M, Craig R (2017) 3D reconstruction of the folded, inhibited form of vertebrate smooth muscle myosin II by single particle analysis. *Biophys J* 112(Suppl 1):266a.
39. Odronitz F, Kollmar M (2008) Comparative genomic analysis of the arthropod muscle myosin heavy chain genes allows ancestral gene reconstruction and reveals a new type of 'partially' processed pseudogene. *BMC Mol Biol* 9:21.
40. Swank DM, et al. (2001) Alternative exon-encoded regions of Drosophila myosin heavy chain modulate ATPase rates and actin sliding velocity. *J Biol Chem* 276:15117–15124.
41. Suggs JA, et al. (2007) Alternative S2 hinge regions of the myosin rod differentially affect muscle function, myofibril dimensions and myosin tail length. *J Mol Biol* 367:1312–1329.
42. Bernstein SI, et al. (1986) Alternative RNA splicing generates transcripts encoding a thorax-specific isoform of Drosophila melanogaster myosin heavy chain. *Mol Cell Biol* 6:2511–2519.
43. Burton PM (2008) Insights from diploblasts; the evolution of mesoderm and muscle. *J Exp Zoolog B Mol Dev Evol* 310:5–14.
44. Seipel K, Schmid V (2005) Evolution of striated muscle: Jellyfish and the origin of triploblasty. *Dev Biol* 282:14–26.
45. Kanzawa N, Sato O, Takano-Ohmuro H, Maruyama K (1993) Sea anemone (Actinia equina) myosin. *Comp Biochem Physiol B* 104:509–514.
46. Simion P, et al. (2017) A large and consistent phylogenomic dataset supports sponges as the sister group to all other animals. *Curr Biol* 27:958–967.
47. Littlewood DTJ (2017) Animal evolution: Last word on sponges-first? *Curr Biol* 27:R259–R261.
48. Bagby RM (1966) The fine structure of myocytes in the sponges Microciona prolifera (Ellis and Solander) and Tedania ignis (Duchassaing and Michelotti). *J Morphol* 118:167–181.
49. Prosser CL (1980) Evolution and diversity of nonstriated muscles. *Vascular Smooth Muscle*, Handbook of Physiology, eds Bohr DF, Somlyo AP, Sparks HV (Am Physiol Soc, Bethesda), pp 635–670.
50. Kanzawa N, Takano-Ohmuro H, Maruyama K (1995) Isolation and characterization of sea sponge myosin. *Zool Sci* 12:765–769.
51. Adl SM, et al. (2005) The new higher level classification of eukaryotes with emphasis on the taxonomy of protists. *J Eukaryot Microbiol* 52:399–451.
52. Sinard JH, Pollard TD (1989) Microinjection into Acanthamoeba castellanii of monoclonal antibodies to myosin-II slows but does not stop cell locomotion. *Cell Motil Cytoskeleton* 12:42–52.
53. Liu X, Hong MS, Shu S, Yu S, Korn ED (2013) Regulation of the filament structure and assembly of Acanthamoeba myosin II by phosphorylation of serines in the heavy-chain nonhelical tailpiece. *Proc Natl Acad Sci USA* 110:E33–E40.
54. Liu X, et al. (2013) Regulation of the actin-activated MgATPase activity of Acanthamoeba myosin II by phosphorylation of serine 639 in motor domain loop 2. *Proc Natl Acad Sci USA* 110:E23–E32.
55. Heissler SM, Liu X, Korn ED, Sellers JR (2013) Kinetic characterization of the ATPase and actin-activated ATPase activities of Acanthamoeba castellanii myosin-2. *J Biol Chem* 288:26709–26720.
56. Pollard TD (1982) Structure and polymerization of Acanthamoeba myosin-II filaments. *J Cell Biol* 95:816–825.
57. Hammer JA, 3rd, Bowers B, Paterson BM, Korn ED (1987) Complete nucleotide sequence and deduced polypeptide sequence of a nonmuscle myosin heavy chain gene from Acanthamoeba: Evidence of a hinge in the rodlike tail. *J Cell Biol* 105:913–925.
58. Sipiczki M (2000) Where does fission yeast sit on the tree of life? *Genome Biol* 1:reviews1011.1–reviews1011.4.
59. Parfrey LW, Lahr DJ, Knoll AH, Katz LA (2011) Estimating the timing of early eukaryotic diversification with multigene molecular clocks. *Proc Natl Acad Sci USA* 108:13624–13629.
60. East DA, Mulvihill DP (2011) Regulation and function of the fission yeast myosins. *J Cell Sci* 124:1383–1390.
61. Bezanilla M, Pollard TD (2000) Myosin-II tails confer unique functions in Schizosaccharomyces pombe: Characterization of a novel myosin-II tail. *Mol Biol Cell* 11:79–91.
62. Baldauf SL, Doolittle WF (1997) Origin and evolution of the slime molds (Mycetozoa). *Proc Natl Acad Sci USA* 94:12007–12012.
63. Egelhoff TT, Manstein DJ, Spudich JA (1990) Complementation of myosin null mutants in Dictyostelium discoideum by direct functional selection. *Dev Biol* 137:359–367.
64. Uchida KS, Kitanishi-Yumura T, Yumura S (2003) Myosin II contributes to the posterior contraction and the anterior extension during the retraction phase in migrating Dictyostelium cells. *J Cell Sci* 116:51–60.
65. Girard KD, Kuo SC, Robinson DN (2006) Dictyostelium myosin II mechanochemistry promotes active behavior of the cortex on long time scales. *Proc Natl Acad Sci USA* 103:2103–2108.
66. Bosgraaf L, van Haastert PJ (2006) The regulation of myosin II in Dictyostelium. *Eur J Cell Biol* 85:969–979.
67. Liu X, et al. (1998) Filament structure as an essential factor for regulation of Dictyostelium myosin by regulatory light chain phosphorylation. *Proc Natl Acad Sci USA* 95:14124–14129.
68. Pasternak C, Flicker PF, Ravid S, Spudich JA (1989) Intermolecular versus intramolecular interactions of Dictyostelium myosin: Possible regulation by heavy chain phosphorylation. *J Cell Biol* 109:203–210.

Lee et al.

www.manaraa.com

69. Steinmetz PR, et al. (2012) Independent evolution of striated muscles in cnidarians and bilaterians. *Nature* 487:231–234.

70. Alamo L, et al. (2016) Conserved intramolecular interactions maintain myosin interacting-heads motifs explaining tarantula muscle super-relaxed state structural basis. *J Mol Biol* 428:1142–1164.

71. Sebé-Pedrós A, Grau-Bové X, Richards TA, Ruiz-Trillo I (2014) Evolution and classification of myosins, a paneukaryotic whole-genome approach. *Genome Biol Evol* 6: 290–305.

72. Korn ED (2000) Coevolution of head, neck, and tail domains of myosin heavy chains. *Proc Natl Acad Sci USA* 97:12559–12564.

73. Pisani D, et al. (2016) Reply to Halanych et al.: Ctenophore misplacement is corroborated by independent datasets. *Proc Natl Acad Sci USA* 113:E948–E949.

74. Boero F, Schierwater B, Piraino S (2007) Cnidarian milestones in metazoan evolution. *Integr Comp Biol* 47:693–700.

75. Yin Z, et al. (2015) Sponge grade body fossil with cellular resolution dating 60 Myr before the Cambrian. *Proc Natl Acad Sci USA* 112:E1453–E1460.

76. Love GD, et al. (2009) Fossil steroids record the appearance of Demospongiae during the Cryogenian period. *Nature* 457:718–721.

77. Ait-Mou Y, et al. (2016) Titin strain contributes to the Frank-Starling law of the heart by structural rearrangements of both thin- and thick-filament proteins. *Proc Natl Acad Sci USA* 113:2306–2311.

78. Reconditi M, et al. (2011) Motion of myosin head domains during activation and force development in skeletal muscle. *Proc Natl Acad Sci USA* 108:7236–7240.

79. Fusi L, Huang Z, Irving M (2015) The conformation of myosin heads in relaxed skeletal muscle: Implications for myosin-based regulation. *Biophys J* 109:783–792.

80. Linari M, et al. (2015) Force generation by skeletal muscle is controlled by mechanosensing in myosin filaments. *Nature* 528:276–279.

81. Huxley HE, Faruqi AR, Kress M, Bordas J, Koch MH (1982) Time-resolved X-ray diffraction studies of the myosin layer-line reflections during muscle contraction. *J Mol Biol* 158:637–684.

82. Zhao FQ, Craig R (2008) Millisecond time-resolved changes occurring in Ca2+-regulated myosin filaments upon relaxation. *J Mol Biol* 381:256–260.

83. Alamo L, et al. (2017) Effects of myosin variants on interacting-heads motif explain distinct hypertrophic and dilated cardiomyopathy phenotypes. *Elife* 6:e24634.

84. Nag S, et al. (2017) The myosin mesa and the basis of hypercontractility caused by hypertrophic cardiomyopathy mutations. *Nat Struct Mol Biol* 24:525–533.

85. Scholey JM, Taylor KA, Kendrick-Jones J (1980) Regulation of non-muscle myosin assembly by calmodulin-dependent light chain kinase. *Nature* 287:233–235.

86. Trybus KM, Lowey S (1984) Conformational states of smooth muscle myosin. Effects of light chain phosphorylation and ionic strength. *J Biol Chem* 259:8564–8571.

87. Somlyo AP, et al. (1983) Ultrastructure, function and composition of smooth muscle. *Ann Biomed Eng* 11:579–588.

88. Horowitz A, Trybus KM, Bowman DS, Fay FS (1994) Antibodies probe for folded monomeric myosin in relaxed and contracted smooth muscle. *J Cell Biol* 126: 1195–1200.

89. Godfraind-De Becker A, Gillis JM (1988) Analysis of the birefringence of the smooth muscle anococcygeus of the rat, at rest and in contraction. I. *J Muscle Res Cell Motil* 9:9–17.

90. Xu JQ, Gillis JM, Craig R (1997) Polymerization of myosin on activation of rat anococcygeus smooth muscle. *J Muscle Res Cell Motil* 18:381–393.

91. Seow CY (2005) Myosin filament assembly in an ever-changing myofilament lattice of smooth muscle. *Am J Physiol Cell Physiol* 289:C1363–C1368.

92. Milton DL, et al. (2011) Direct evidence for functional smooth muscle myosin II in the 10S self-inhibited monomeric conformation in airway smooth muscle cells. *Proc Natl Acad Sci USA* 108:1421–1426.

93. Katoh T, Konishi K, Yazawa M (1998) Skeletal muscle myosin monomer in equilibrium with filaments forms a folded conformation. *J Biol Chem* 273:11436–11439.

94. Saad AD, Pardee JD, Fischman DA (1986) Dynamic exchange of myosin molecules between thick filaments. *Proc Natl Acad Sci USA* 83:9483–9487.

95. Johnson CS, McKenna NM, Wang Y (1988) Association of microinjected myosin and its subfragments with myofibrils in living muscle cells. *J Cell Biol* 107:2213–2221.

96. Ankrett RJ, Rowe AJ, Cross RA, Kendrick-Jones J, Bagshaw CR (1991) A folded (10 S) conformer of myosin from a striated muscle and its implications for regulation of ATPase activity. *J Mol Biol* 217:323–335.

97. Hellerschmied D, Clausen T (2014) Myosin chaperones. *Curr Opin Struct Biol* 25:9–15.

98. Srikakulam R, Winkelmann DA (2004) Chaperone-mediated folding and assembly of myosin in striated muscle. *J Cell Sci* 117:641–652.

99. Alberts B, et al. (2007) *Molecular Biology of the Cell* (Garland Science, New York), 5th Ed.

100. Mouw JK, Ou G, Weaver VM (2014) Extracellular matrix assembly: A multiscale deconstruction. *Nat Rev Mol Cell Biol* 15:771–785.

101. Josephson RK, Malamud JG, Stokes DR (2000) Power output by an asynchronous flight muscle from a beetle. *J Exp Biol* 203:2667–2689.

102. Hu Z, Taylor DW, Reedy MK, Edwards RJ, Taylor KA (2016) Structure of myosin filaments from relaxed Lethocerus flight muscle by cryo-EM at 6 Å resolution. *Sci Adv* 2:e1600058.

103. Fee L, Lin W, Qiu F, Edwards RJ (2017) Myosin II sequences for Lethocerus indicus. *J Muscle Res Cell Motil* 38:193–200.

104. Romeralo M, Escalante R, Baldauf SL (2012) Evolution and diversity of dictyostelid social amoebae. *Protist* 163:327–343.

105. Griffith LM, Downs SM, Spudich JA (1987) Myosin light chain kinase and myosin light chain phosphatase from Dictyostelium: Effects of reversible phosphorylation on myosin structure and function. *J Cell Biol* 104:1309–1323.

106. Dickinson DJ, Nelson WJ, Weis WI (2012) An epithelial tissue in Dictyostelium challenges the traditional origin of metazoan multicellularity. *BioEssays* 34:833–840.

107. Pollard LW, et al. (2017) Fission yeast myosin Myo2 is down-regulated in actin affinity by light chain phosphorylation. *Proc Natl Acad Sci USA* 114:E7236–E7244.

108. Brunet T, et al. (2016) The evolutionary origin of bilaterian smooth and striated myocytes. *Elife* 5:e19607.

109. Sellers JR (2000) Myosins: A diverse superfamily. *Biochim Biophys Acta* 1496:3–22.

110. Hooijman P, Stewart MA, Cooke R (2011) A new state of cardiac myosin with very slow ATP turnover: A potential cardioprotective mechanism in the heart. *Biophys J* 100:1969–1976.

111. Naber N, Cooke R, Pate E (2011) Slow myosin ATP turnover in the super-relaxed state in tarantula muscle. *J Mol Biol* 411:943–950.

112. Pufall MA, Graves BJ (2002) Autoinhibitory domains: Modular effectors of cellular regulation. *Annu Rev Cell Dev Biol* 18:421–462.

113. Trudeau T, et al. (2013) Structure and intrinsic disorder in protein autoinhibition. *Structure* 21:332–341.

114. Heissler SM, Sellers JR (2016) Various themes of myosin regulation. *J Mol Biol* 428: 1927–1946.

115. Trybus KM (2008) Myosin V from head to tail. *Cell Mol Life Sci* 65:1378–1389.

116. Li XD, Mabuchi K, Ikebe R, Ikebe M (2004) Ca2+-induced activation of ATPase activity of myosin Va is accompanied with a large conformational change. *Biochem Biophys Res Commun* 315:538–545.

117. Wang F, et al. (2004) Regulated conformation of myosin V. *J Biol Chem* 279: 2333–2336.

118. Krementsov DN, Krementsova EB, Trybus KM (2004) Myosin V: Regulation by calcium, calmodulin, and the tail domain. *J Cell Biol* 164:877–886.

119. Umeki N, et al. (2009) The tail binds to the head-neck domain, inhibiting ATPase activity of myosin VIIA. *Proc Natl Acad Sci USA* 106:8483–8488.

120. Sakai T, et al. (2015) Structure and regulation of the movement of human myosin VIIA. *J Biol Chem* 290:17587–17598.

121. Umeki N, et al. (2011) Phospholipid-dependent regulation of the motor activity of myosin X. *Nat Struct Mol Biol* 18:783–788.

122. Verhey KJ, Hammond JW (2009) Traffic control: Regulation of kinesin motors. *Nat Rev Mol Cell Biol* 10:765–777.

123. Torisawa T, et al. (2014) Autoinhibition and cooperative activation mechanisms of cytoplasmic dynein. *Nat Cell Biol* 16:1118–1124.

124. Agafonov R, Wilson C, Biswas S, Kern D (2015) Regulation of kinases: 1 billion years of evolution. *Biophys J* 108(Suppl 1):381a.

125. Ikebe M, Hartshorne DJ (1985) Effects of Ca2+ on the conformation and enzymatic activity of smooth muscle myosin. *J Biol Chem* 260:13146–13153.

126. Liu X, Shu S, Yamashita RA, Xu Y, Korn ED (2000) Chimeras of Dictyostelium myosin II head and neck domains with Acanthamoeba or chicken smooth muscle myosin II tail domain have greatly increased and unregulated actin-dependent MgATPase activity. *Proc Natl Acad Sci USA* 97:12553–12558.

127. Swank DM, Wells L, Kronert WA, Morrill GE, Bernstein SI (2000) Determining structure/function relationships for sarcomeric myosin heavy chain by genetic and transgenic manipulation of Drosophila. *Microsc Res Tech* 50:430–442.

128. Kronert WA, Dambacher CM, Knowles AF, Swank DM, Bernstein SI (2008) Alternative relay domains of Drosophila melanogaster myosin differentially affect ATPase activity, in vitro motility, myofibril structure and muscle function. *J Mol Biol* 379: 443–456.

129. Burgess SA, Walker ML, Thirumurugan K, Trinick J, Knight PJ (2004) Use of negative stain and single-particle image processing to explore dynamic properties of flexible macromolecules. *J Struct Biol* 147:247–258.

130. Elliott A, Offer G (1978) Shape and flexibility of the myosin molecule. *J Mol Biol* 123: 505–519.

131. Tang G, et al. (2007) EMAN2: An extensible image processing suite for electron microscopy. *J Struct Biol* 157:38–46.

132. Scheres SH (2012) A Bayesian view on cryo-EM structure determination. *J Mol Biol* 415:406–418.

133. UniProt Consortium (2015) UniProt: A hub for protein information. *Nucleic Acids Res* 43:D204–D212.

134. Waterhouse AM, Procter JB, Martin DM, Clamp M, Barton GJ (2009) Jalview Version 2–A multiple sequence alignment editor and analysis workbench. *Bioinformatics* 25: 1189–1191.

135. Hooper SL, Thuma JB (2005) Invertebrate muscles: Muscle specific genes and proteins. *Physiol Rev* 85:1001–1060.

136. Cheney RE, Riley MA, Mooseker MS (1993) Phylogenetic analysis of the myosin superfamily. *Cell Motil Cytoskeleton* 24:215–223.

137. Goodson HV, Spudich JA (1993) Molecular evolution of the myosin family: Relationships derived from comparisons of amino acid sequences. *Proc Natl Acad Sci USA* 90:659–663.

138. Edgar RC (2004) MUSCLE: Multiple sequence alignment with high accuracy and high throughput. *Nucleic Acids Res* 32:1792–1797.

www.manaraa.com